and appears to converge to a smaller range of values as the maximal affinity is approached. For this series of plasmepsin II inhibitors based upon the allophenylnorstatine scaffold, the highest affinity was achieved with a binding enthalpy of −4.5 kcal/mol and an entropic contribution ($-T\Delta S$) of −8.8 kcal/mol.

The data in Figure 1 clearly demonstrates the importance of balancing enthalpic and entropic contributions in order to maximize binding affinity and illustrates important steps in the design process. As enthalpic interactions are more difficult to engineer, enthalpically driven hits are usually easier to optimize than entropically driven ones; i.e. it is less costly energetically to introduce hydrophobic groups. A calorimetric characterization of hits identified by screening or any other method should allow the designer to recognize the nature of the forces by which the hits bind to the target. This step is crucial at these early stages, because it allows separation of those molecules that bind because they are excluded from the solvent from those that bind because they establish favorable interactions with the target. It is at the earlier stages where the spread of enthalpy/entropy combinations is maximal and where a careful decision needs to be made. It is always advantageous to choose compounds that establish good interactions with the target and thermodynamic dissection provides that information. Further down the optimization road, thermodynamic dissection indicates if the process is driven within a reasonable pathway, avoiding thermodynamic extremes that sooner or later lead the process to a roadblock and sometimes a dead end. Obviously, this task is facilitated if it is supplemented by algorithms able to predict the enthalpic or entropic consequences of introducing different chemical functionalities in the scaffold under optimization.

Acknowledgment

This work was supported by grants from the National Institutes of Health GM 57144 and GM56550 and the National Science Foundation MCB0131241.

References

1. Lipinski C.A., Lombardo F., Dominy B.W., Feeney P.J. (1997) Experimental and computational approaches to estimate solubility and permeability in drug discovery and development settings. Adv Drug Delivery Rev;23:3–25.
2. Lipinski C.A. (2000) Drug-like properties and the causes of poor solubility and poor permeability. J Pharmacol and Toxicol Methods;44:235–249.
3. Ohtaka H., Muzammil S., Schon A., Velazquez-Campoy A., Vega S., Freire E. (2004) Thermodynamic rules for the design of high affinity HIV-1 protease inhibitors with adaptability to mutations and high selectivity towards unwanted targets. Int J Biochem Cell Biol;36:1787–1799.
4. Ohtaka H., Freire E. (2005) Adaptive Inhibitors of the HIV-1 protease. Progr Biophys Mol Biol;88:193–208.
5. Carbonell T., Freire E. (2005) Binding thermodynamics of statins to HMG-CoA reductase. Biochemistry;44:11741–11748.
6. Luque I., Freire E. (2002) Structural parameterization of the binding enthalpy of small ligands. Proteins;49:181–190.
7. Nezami A., Luque I., Kimura T., Kiso Y., Freire E. (2002) Identification and characterization of allophenylnorstatine-based inhibitors of plasmepsin II, an anti-malarial target. Biochemistry;41:2273–2280.
8. Nezami A., Kimura T., Hidaka K., Kiso A., Liu J., Kiso Y., Goldberg D.E., Freire E. (2003) High affinity inhibition of a family of *Plasmodium falciparum* proteases by a designed adaptive inhibitor. Biochemistry;42:8459–8464.
9. Cabani S., Gianni P., Mollica V., Lepori L. (1981) Group contributions to the thermodynamic properties of non-ionic organic solutes in dilute aqueous solution. J Solution Chem;10:563–595.

Available online at www.sciencedirect.com
SCIENCE DIRECT
Microbes and Infection 7 (2005) 385–390
Microbes and Infection
www.elsevier.com/locate/micinf

Original article

Unique characteristics of HIV-1 Vif expression

Huaqing Wang [a,b], Akiko Sakurai [b], Boonruang Khamsri [b], Tsuneo Uchiyama [b], Hongxi Gu [a], Akio Adachi [b], Mikako Fujita [b,*]

[a] *Department of Microbiology, Harbin Medical University, Harbin 150086, People's Republic of China*
[b] *Department of Virology, Institute of Health Biosciences, The University of Tokushima Graduate School, Tokushima 770-8503, Japan*

Received 16 October 2004; accepted 12 November 2004

Available online 19 March 2005

Abstract

We examined the steady-state expression in cells of four accessory proteins of human immunodeficiency virus type 1 (HIV-1). For this purpose, a series of single gene expression vectors for these viral proteins were constructed and were monitored for their production by transfection. Among them, the expression level of Vif was found to be lowest in both the absence and presence of APOBEC3G. In addition, we noticed the presence of its truncated form, which was not observed for the other accessory proteins. When a subgenomic vector was used for transfection, authentic and several small forms of Vif were produced. By mutational analysis, these forms were demonstrated to be mutant Vif proteins translated from M^{8}, M^{16} and M^{29}. When a full-length molecular clone was used, the smaller versions of Vif were hardly observed. Functional analysis of these mutant Vif proteins showed that they are incapable of modulating viral infectivity. The results described above, i.e. the low steady-state expression and the presence of truncated forms, represent the unique characteristics of HIV-1 Vif.

Keywords: HIV-1; Vif; APOBEC3G; Accessory protein

1. Introduction

Four accessory proteins of human immunodeficiency virus type 1 (HIV-1) are known to modulate viral infectivity and various functions of target cells [1]. Vif, one of these proteins, is encoded by the gene that is conserved in all known primate immunodeficiency viruses [2]. It has a critical role in conferring infectivity on progeny virions in a producer cell-dependent manner [3–6]. Virions produced in non-permissive cells, such as primary cells of lymphocytic or monocytic origin and a limited number of cell lines like H9, are unable to replicate in any kinds of target cells. Recent works have demonstrated that Vif counteracts anti-viral activity of human cytidine deaminase APOBEC3G present in non-permissive cells [7–15]. The precise molecular mechanism for this activity of Vif, however, is still controversial [16] and remains to be elucidated.

We have previously shown that Vif is rapidly decayed in cells in both the absence and presence of APOBEC3G, and that the expression of Vif to an excessive level is inhibitory to viral replication [17]. The fragile nature of Vif was unique among the accessory proteins and was mediated, at least in part, by the host proteasome system [18]. In the present report, to determine whether the expression of Vif is maintained to be uniquely low in cells in the absence of the other viral factors, the four accessory genes of HIV-1 were separately cloned into expression vector with tag, and examined for their steady-state expression level. During the course of this comparative study, we detected a truncated form of Vif, but no extra versions were observed for the other accessory proteins. We, therefore, examined the expression pattern of Vif from a subgenomic clone, and found two other small forms. Mutational and functional analyses of the three small Vif proteins were also carried out in this study.

2. Materials and methods

2.1. Plasmids

2.1.1. Full-length molecular clones

A full-length molecular clone pNL432 (GenBank Accession no. AF324493) was used for production of wild-type

* Corresponding author. Tel.: +81 88 633 9232; fax: +81 88 633 7080.
E-mail address: mfujita@basic.med.tokushima-u.ac.jp (M. Fujita).

1286-4579/$ - see front matter © 2005 Elsevier SAS. All rights reserved.
doi:10.1016/j.micinf.2004.11.010

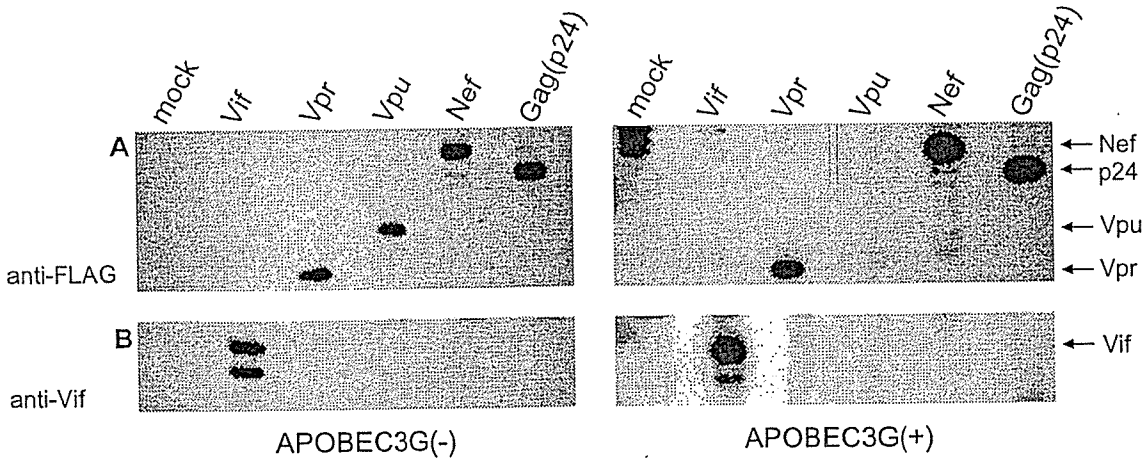

Fig. 1. Production of HIV-1 (NL432) accessory proteins by expression vector pSG-FLAG. 293T cells were transfected with 10 μg of pSG-FLAG vectors with (APOBEC3G(+)) or without (APOBEC3G(–)) 1 μg of pcDNA-APO3G (expression vector for APOBEC3G) [9]. Cells were lysed in Laemmli sample buffer at 48 h post-transfection for Western blot analysis. Each lane contained 50 ng of protein. The Abs used here were anti-FLAG M2 monoclonal Ab (panels A) and anti-Vif peptide Ab [22] (panels B). An expression vector for Gag-p24, designated pSG-Gag (p24) cFLAG [18], was used for control. Mock, pSG5.

(wt) infectious virus [19]. Frame-shift mutants of pNL432, designated pNL-Nd [20,21], pNL-Kp [20] and pNL-NdKp [22], were used for production of *vif*-minus, *env*-minus and *vif/env* double-minus viruses, respectively.

2.1.2. Subgenomic vectors

A subgenomic expression vector, designated pNL-A1S, was constructed from pNL-A1 [23]. For easy insertion of DNA fragments from pNL432 [19], it has a unique *Sma*I site (Fig. 2B) newly generated by the QuikChange site-directed mutagenesis kit (Stratagene, La Jolla, CA, USA). Various subgenomic expression vectors for wt and mutant Vif proteins described below were constructed by insertion of PCR-amplified *vif* sequences having *Sma*I and *Eco*RI sites at 5′ and 3′ ends, respectively, into pNL-A1S (Fig. 2B). PCR templates for construction of pNL-A1S-fWT, pNL-A1S-Nd, pNL-A1S-fM16A, pNL-A1S-fM8/16A and pNL-A1S-fM8/16/29A were pNL432 [19], pNL-Nd [20,21], pNL-fM16A, pNL-fM8/16A and pNL-fM8/16/29A, respectively. Clones pNL-fM16A, pNL-fM8/16A, and pNL-fM8/16/29A are mutants of pNL432 carrying M16A, M8/16A and M8/16/29A mutations, respectively (Fig. 3A).

2.1.3. Expression vectors for a single gene

Vectors pcDNA-APO3G [9] and pCMV-G [24] were used to express APOBEC3G and vesicular stomatitis virus G protein (VSV-G), respectively. Expression vectors for wt and mutant Vif proteins, designated pSG-Vif, pSG-fΔ7, pSG-fΔ15 and pSG-fΔ28, were constructed by insertion of PCR-amplified *vif* sequences having *Eco*RI and *Bam*HI sites at 5′ and 3′ ends, respectively, into pSG5 (Stratagene). As template for PCR, pNL432 [19] was used. An expression vector for wt Vif tagged with FLAG at the C-terminus, designated pSG-Vif cFLAG, was constructed in the same way as for pSG-Gag (p24) cFLAG [18]. Expression vectors for the other accessory proteins tagged with FLAG at the C-terminus, designated pSG-Vpr cFLAG, pSG-Vpu cFLAG and pSG-Nef

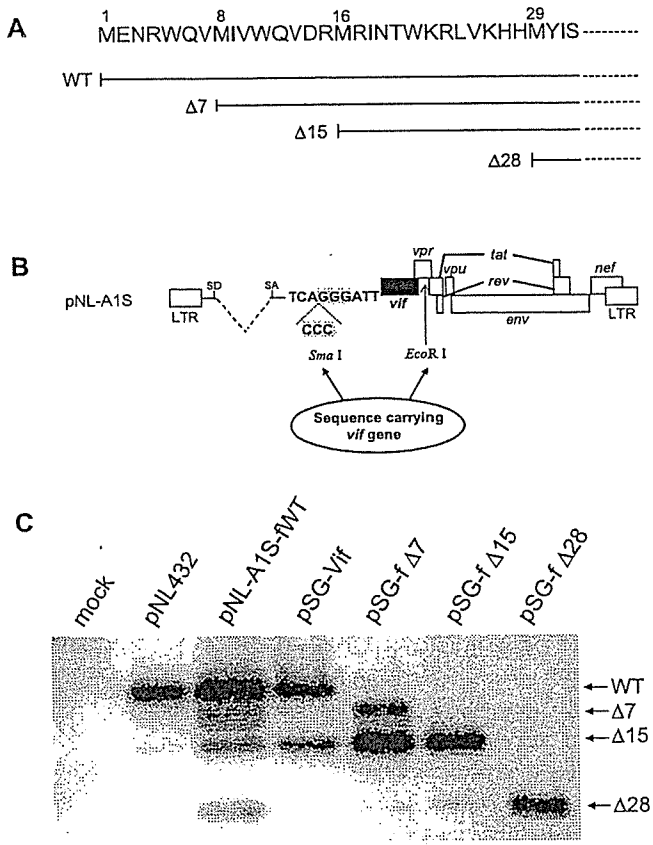

Fig. 2. Expression of HIV-1 (NL432) Vif-related proteins by various clones. (A) Structure of three putative mutants of Vif. Mutants Δ7, Δ15, and Δ28 lack N-terminal 7, 15 and 28 amino acids, respectively. (B) Structure of expression vector for Vif (pNL-A1S). Vector pNL-A1S has a new and unique *Sma*I site (relative to parental clone pNL-A1) for cloning, as indicated. (C) Monitoring of Vif-related proteins by Western blot analysis. 293T cells were transfected with 10 μg of various vectors, as indicated, and cell lysates were prepared by CHAPS buffer at 48 h post-transfection. Anti-Vif peptide Ab was used for detection as previously described [22]. Each lane contained 50 ng of protein, execpt for the lane for pNL-A1S-fWT (5 ng of protein). Mock, pUC19.

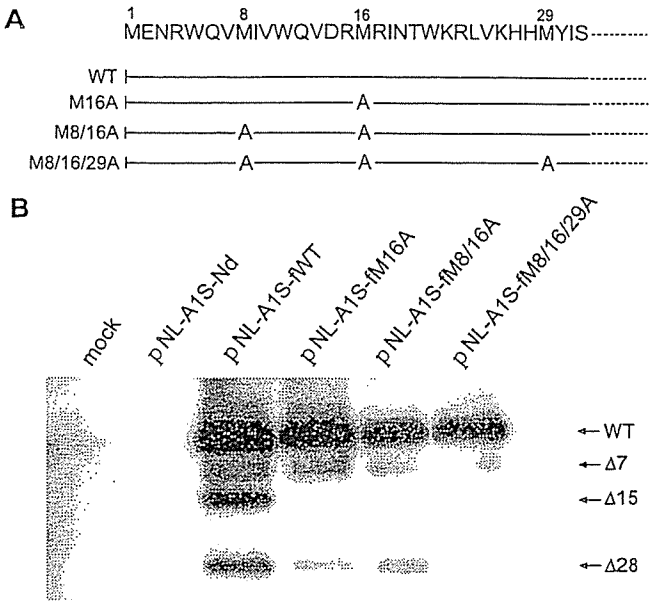

Fig. 3. Expression of various species of HIV-1 (NL432) Vif proteins by subgenomic pNL-A1S constructs. (A) N-terminal amino acid sequence of mutant Vif proteins. Mutant clones have alanine residues instead of methionines, as indicated. (B) Monitoring of Vif-related proteins expressed by subgenomic pNL-A1S constructs. 293T cells were transfected with 10 μg of various vectors, as indicated, and cell lysates were prepared in Laemmli sample buffer at 48 h post-transfection. Anti-Vif peptide Ab was used for detection, as previously described [22]. Each lane contained 5 ng of protein. Mock, pUC19.

cFLAG, were constructed by replacement of the *gag* gene of pSG-Gag (p24) cFLAG [18] with PCR-amplified accessory gene sequences having *Eco*RI and *Xho*I sites at 5′ and 3′ ends, respectively. As template for PCR, pNL432 [19] was used.

2.2. Cells

H9 [25] and 293T [26] cells were cultured in RPMI-1640 medium supplemented with 10% heat-inactivated fetal bovine serum (FBS), and in Eagle's minimal essential medium supplemented with 10% heat-inactivated FBS, respectively. MAGI cells [27] were cultured as for 293T cells in the presence of 0.2 mg/ml of G418 and 0.1 mg/ml of hygromycin B.

2.3. Transfection and reverse transcriptase (RT) assay

For transfection of 293T cells, the calcium-phosphate coprecipitation method was used as previously described [19]. Virus production in the culture supernatants was monitored by RT activity as previously described [28].

2.4. Western immunoblotting

Cell lysates for Western blotting analysis were prepared by CHAPS/DOC [28] or Laemmli's sample buffer [18] as previously described. Samples were resolved by SDS-PAGE followed by electrophoretic transfer to polyvinylidene fluoride membranes. The membranes were treated with anti-FLAG M2 monoclonal antibody (Ab) (SIGMA-ALDRICH Corp., St. Louis, MO, USA) or anti-Vif peptide Ab [22], and visualized with the ECL plus Western Blotting Detection System (Amersham Biosciences UK Limited, Buckinghamshire, UK) as previously described [29,30].

2.5. MAGI assay

To determine the infectivity of virions, MAGI assay was performed as previously described [27].

3. Results

3.1. Low expression level of Vif protein in cells

Recent work by ourselves has shown that Vif expressed from viral full-genome is degraded rapidly and maintained to be at low level in cells by proteasome [18], and that this unstable nature of Vif was unique among the accessory proteins [18]. We asked, in a quantitative and comparable manner, whether the expression level of Vif is uniquely low in cells in the absence of the other viral proteins. For this purpose, the four HIV-1 accessory genes, *vif*, *vpr*, *vpu* and *nef*, were separately cloned into expression vector pSG5-FLAG tag, and four expression vectors for each accessory protein, designated pSG-Vif cFLAG, pSG-Vpr cFLAG, pSG-Vpu cFLAG and pSG-Nef cFLAG were constructed. These clones were then transfected into permissive 293T cells with or without APOBEC3G expression vector pcDNA-APO3G [9] and monitored for their expression by Western blot analysis using anti-FLAG antibody. Laemmli's sample buffer was used to prepare cell lysates for analysis, since Vif was quite refractory to CHAPS/DOC buffer [28,31]. As shown in Fig. 1A, regardless of the presence or absence of APOBEC3G, no Vif was detected, in contrast to the results for Vpr and Nef, when anti-FLAG Ab was used. Worthy of note, in the presence of APOBEC3G, Vpu was not detected at all. In the absence of APOBEC3G, Vpu was expressed at a level similar to that of Vpr. We wished to examine the expression of Vif using Ab other than anti-FLAG Ab. As shown in Fig. 1B, when the same blots in Fig. 1A were re-probed with anti-Vif peptide Ab, two Vif-related bands (~23 and ~21 kDa) appeared both in the absence and presence of APOBEC3G. These probably represented authentic and truncated forms of Vif.

The results described here indicated that Vif is certainly expressed in cells at a relatively low level. Another important finding was the presence of the truncated version of Vif.

3.2. Truncated forms of Vif proteins

We assumed that, on the basis of its size, the truncated form of Vif is a mutant Vif translated from M^{16}, as shown in Fig. 2A. To verify this hypothesis, expression vectors of wt Vif and its mutants, Δ7, Δ15 and Δ28, based on pSG5 (pSG-Vif, pSG-fΔ7, pSG-fΔ15 and pSG-fΔ28), were constructed (Fig. 2A) and used for monitoring of their products in cells upon transfection. A subgenomic expression vector, desig-

nated pNL-A1S-fWT, was also constructed (Fig. 2B) and used, because the expression level of Vif by this vector was expected to be very high [23]. The vectors constructed were then introduced into 293T cells and examined for the expression pattern of Vif by Western blotting technique. As shown in Fig. 2C, while wt full-length clone pNL432 generated a distinct and single Vif, the subgenomic clone pNL-A1S-fWT produced several Vif proteins recognizable by anti-Vif peptide Ab. The mutant pSG constructs expressed Vif-related proteins well-anticipated by our assumption. It was, therefore, not unreasonable to conclude that there are three mutant Vif proteins starting from M^8, M^{16} and M^{29}. To prove this, three methionines present in the N-terminal region of Vif (Fig. 3A) were changed to alanines, and the mutants constructed were examined for their products upon transfection (pNL-A1S series in Fig. 3B). The results obtained were in good agreement with our prediction. Mutants pNL-A1S-fM16A, pNL-A1S-fM8/16A and pNL-A1S-fM8/16/29A did not produce a central major band (Δ15). Mutant pNL-A1S-fM8/16/29A did not express the smallest band (Δ28) at all. In addition, one of the faint bands (Δ7) just below the authentic Vif appeared to disappear for mutants pNL-A1S-fM8/16A and pNL-A1S-fM8/16/29A. The data described above were reproduced for the samples prepared in the presence of APOBEC3G (data not shown). Furthermore, consistently with the data described above, the M16A mutant of pSG-construct did not produce the major Δ15 band upon transfection (data not shown).

3.3. Biological activity of small versions of Vif proteins

We asked ourselves whether truncated forms of Vif were able to confer infectivity on progeny virions. *Vif*-minus full-length clone pNL-Nd [20,21] and expression vectors of Vif or its mutants (pSG-Vif, pSG-fΔ7, pSG-fΔ15 and pSG-fΔ28) with or without pcDNA-APO3G [9] were co-transfected into 293T cells, and the effects of various Vif pro-

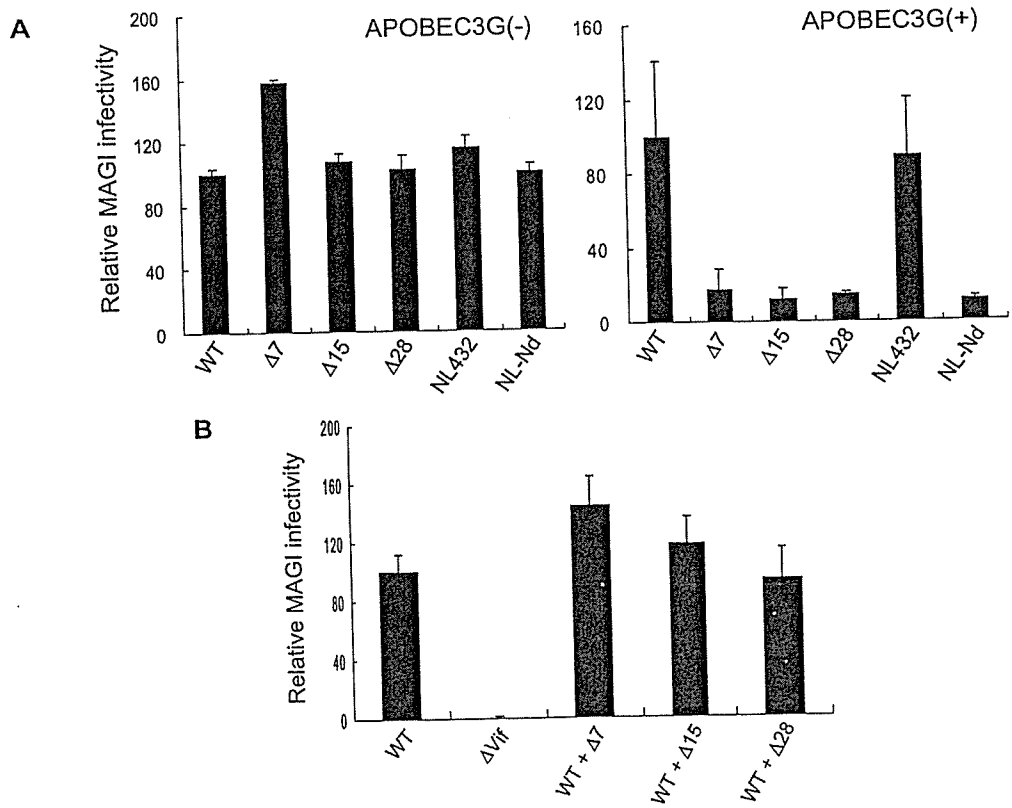

Fig. 4. Biological evaluation of various species of HIV-1 (NL432) Vif. (A) Ability of mutant Vif proteins to confer infectivity on progeny virions. 293T cells were triply transfected with 2.5 μg of pNL-Nd [20,21], 7.5 μg of expression vector (pSG-Vif (WT), pSG-fΔ7, pSG-fΔ15 or pSG-fΔ28) and 1 μg of pcDNA-APO3G (expression vector of APOBEC3G) [9] (APOBEC3G(+)), or dually transfected with the former two clones (APOBEC3G(–)). At 48 h post-transfection, culture supernatants were harvested for virus samples as previously described [29]. As control for virus samples, culture supernatants prepared from 293T cells transfected with wt pNL432 [19] or ΔVif mutant pNL-Nd [20,21] with (APOBEC3G(+)) or without pcDNA-APO3G [9] (APOBEC3G(–)) were used. The prepared virus samples were inoculated into MAGI cells, and infectivity was determined as previously described [27]. MAGI infectivity was normalized by RT activity and shown as relative values. (B) Effects of mutant Vif proteins on viral infectivity. 293T cells were co-transfected with 1.3 μg of *env*-minus full-length clone pNL-Kp [20], 1.3 μg of pCMV-G (expression vector of VSV-G) [24], 7.5 μg of expression vector (empty vector pSG5, pSG-fΔ7, pSG-fΔ15 or pSG-fΔ28), and 1 μg of pcDNA-APO3G (expression vector of APOBEC3G). Under these conditions, similar amounts of wt Vif and Δ15 mutant were expressed from pNL-Kp and pSG-fΔ15, respectively. Virus samples were harvested at 48 h post-transfection, and their infectivity was determined by MAGI assay, as described in (A). MAGI infectivity was normalized by RT activity and shown as relative values. WT, pNL-Kp + pSG5; ΔVif, pNL-NdKp + pSG5; WT + Δ7, pNL-Kp + pSGfΔ7; WT + Δ15, pNL-Kp + pSGfΔ15; WT + Δ28, pNL-Kp + pSGfΔ28. A full-length clone pNL-NdKp [22] was *vif/env* double-minus, and served as a negative control for pNL-Kp [20].

teins on viral infectivity were examined. As shown in Fig. 4A, in the absence of APOBEC3G, all virus samples showed similar MAGI infectivity, as expected. In the presence of APOBEC3G, while wt Vif conferred an infectivity on virions comparable to that of wt virus NL432, none of the truncated forms of Vif did like ΔVif mutant virus NL-Nd. We then examined whether truncated forms of Vif had negative effects on infectivity of virions. *Env*-minus full-length clone pNL-Kp [20], one of the expression vectors for Vif mutants as above, an expression vector of VSV-G protein pCMV-G [24] and pcDNA-APO3G [9] were co-transfected into 293T cells, and the infectivity of viruses produced at 2 days post-transfection was determined. As shown in Fig. 4B, no truncated forms of Vif exhibited any significant negative effects on viral infectivity.

4. Discussion

One of the major findings in this study is that the expression of Vif is consistently controlled to be low (Fig. 1). We have previously proposed a mechanism for this observation, that is, proteasome degradation [18]. Vif was much more rapidly degraded than any other accessory proteins and kept low in cells. The other possible explanation for the restricted expression of Vif is related to mRNA. Expression of mRNA for Vif was reported to be maintained to be limited [32]. The unstabilness of mRNA for Vpu was also reported [32], and this could cause the lower expression level of Vpu compared with that of Nef (Fig. 1). In this context, the lack of detectable expression of Vpu in the presence of APOBEC3G (Fig. 1) was intriguing. The plausible mechanism for the down-regulation of Vpu could be the introduction of mutations to mRNA for Vpu by the cytidine deaminase activity of APOBEC3G and/or the enhancement of degradation of Vpu by APOBEC3G.

Another major finding in this report is the production of truncated forms of Vif (Figs. 1–3). We showed evidence here by mutational analysis that these Vif-related proteins are translated from M^8, M^{16} or M^{29} (Fig. 3). To the best of our knowledge, this is the first report that shows the initiation of translation of HIV-1 proteins at a methionine codon other than M^1. Of note, the expression pattern of the Vif proteins varied depending on the clones used. Clones pSG-Vif (single gene) and pNL-A1S-fWT (subgenome) expressed one (Δ15) and three (Δ7, Δ15 and Δ28) Vif proteins, respectively (Figs. 1–3). Full-genomic pNL432 appeared not to express any small forms of Vif (Fig. 2). The molecular basis for this observation remains to be elucidated. It is also important to determine whether the truncated Vif proteins described here are biologically active. Our functional analysis in this report showed that small forms of Vif are biologically inactive (Fig. 4). It is still possible, however that these Vif proteins affect the replication of virus by unknown mechanisms.

Acknowledgements

We are indebted to Dr. Klaus Strebel (NIAID, NIH, USA) for donating pcDNA-APO3G. We thank Ms. Kazuko Yoshida for editorial assistance. This work was supported by a Grant-in-Aid for Scientific Research (C) (15590420) and a Grant-in-Aid for Scientific Research (B) (14370103) from the Japan Society for the Promotion of Science, and a Grant-in-Aid for Scientific Research on Priority Areas (2) (16017270) from the Ministry of Education, Culture, Sports, Science and Technology of Japan, and a Health Sciences Research Grant from the Ministry of Health, Labour and Welfare of Japan. H.W. is a Visiting Scientist supported by the Chinese and Japanese governments.

References

[1] E.O. Freed, M.A. Martin, HIVs and their replication, fourth ed, in: D.M. Knipe, P.M. Howley (Eds.), Fields Virology, 2, Lippincott Williams and Wilkins, Philadelphia, 2001, pp. 1971–2041.

[2] R.J. Miller, J.S. Cairns, S. Bridges, N. Sarver, Human immunodeficiency virus and AIDS: insights from animal lentiviruses, J. Virol. 74 (2000) 7187–7195.

[3] S. Bour, K. Strebel, HIV accessory proteins: multifunctional components of a complex system, Adv. Pharmacol. 48 (2000) 75–120.

[4] B.R. Cullen, HIV-1 auxiliary proteins: making connections in a dying cell, Cell 93 (1998) 685–692.

[5] M. Emerman, M.H. Malim, HIV-1 regulatory/accessory genes: keys to unraveling viral and host cell biology, Science 280 (1998) 1880–1884.

[6] R. Inubushi, M. Tamaki, R. Shimano, A.H. Koyama, H. Akari, A. Adachi, Functional roles of HIV accessory proteins for viral replication, Int. J. Mol. Med. 2 (1998) 429–433.

[7] A.M. Sheehy, N.C. Gaddis, J.D. Choi, M.H. Malim, Isolation of a human gene that inhibits HIV-1 infection and is suppressed by the viral Vif protein, Nature 418 (2002) 645–650.

[8] K. Stopak, C. de Noronha, W. Yonemoto, W.C. Greene, HIV-1 Vif blocks the antiviral activity of APOBEC3G by impairing both its translation and intracellular stability, Mol. Cell 12 (2003) 591–601.

[9] S. Kao, M.A. Khan, E. Miyagi, R. Plishka, A. Buckler-White, K. Strebel, The human immunodeficiency virus type 1 Vif protein reduces intracellular expression and inhibits packaging of APOBEC3G (CEM15), a cellular inhibitor of virus infectivity, J. Virol. 77 (2003) 11398–11407.

[10] R. Mariani, D. Chen, B. Schrofelbauer, F. Navarro, R. Konig, B. Bollman, C. Munk, H. Nymark-McMahon, N.R. Landau, Species-specific exclusion of APOBEC3G from HIV-1 virions by Vif, Cell 114 (2003) 21–31.

[11] M. Marin, K.M. Rose, S.L. Kozak, D. Kabat, HIV-1 Vif protein binds the editing enzyme APOBEC3G and induces its degradation, Nat. Med. 9 (2003) 1398–1403.

[12] A.M. Sheehy, N.C. Gaddis, M.H. Malim, The antiretroviral enzyme APOBEC3G is degraded by the proteasome in response to HIV-1 Vif, Nat. Med. 9 (2003) 1404–1407.

[13] X. Yu, Y. Yu, B. Liu, K. Luo, W. Kong, P. Mao, X.F. Yu, Induction of APOBEC3G ubiquitination and degradation by an HIV-1 Vif-Cul5-SCF complex, Science 302 (2003) 1056–1060.

[14] S.G. Conticello, R.S. Harris, M.S. Neuberger, The Vif protein of HIV triggers degradation of the human antiretroviral DNA deaminase APOBEC3G, Curr. Biol. 13 (2003) 2009–2013.

[15] A. Mehle, B. Strack, P. Ancuta, C. Zhang, M. McPike, D. Gabuzuda, Vif overcomes the innate antiviral activity of APOBEC3G by promoting its degradation in the ubiquitin-proteasome pathway, J. Biol. Chem. 279 (2004) 7792–7798.

[16] S. Kao, E. Miyagi, M.A. Khan, H. Takeuchi, S. Opi, R. Goila-Gaur, K. Strebel, Production of infectious human immunodeficiency virus type 1 does not require depletion of APOBEC3G from virus-producing cells, Retrovirology 1 (2004) 27.

[17] H. Akari, M. Fujita, S. Kao, M.A. Khan, M. Shehu-Xhilaga, A. Adachi, K. Strebel, High level expression of human immunodeficiency virus type-1 Vif inhibits viral infectivity by modulating proteolytic processing of the Gag precursor at the p2/NC processing site, J. Biol. Chem. 279 (2004) 12355–12362.

[18] M. Fujita, H. Akari, A. Sakurai, A. Yoshida, T. Chiba, K. Tanaka, K. Strebel, A. Adachi, Expression of HIV-1 accessory protein Vif is controlled uniquely to be low and optimal by proteasome degradation, Microbes Infect. 6 (2004) 791–798.

[19] A. Adachi, H.E. Gendelman, S. Koenig, T. Folks, R. Willey, A. Rabson, M.A. Martin, 1986. Production of acquired immunodeficiency syndrome-associated retrovirus in human and nonhuman cells transfected with an infectious molecular clone, J. Virol. 59 (1986) 284–291.

[20] A. Adachi, N. Ono, H. Sakai, K. Ogawa, R. Shibata, T. Kiyomasu, H. Masuike, S. Ueda, Generation and characterization of the human immunodeficiency virus type 1 mutants, Arch. Virol. 117 (1991) 45–58.

[21] H. Sakai, R. Shibata, J.I. Sakuragi, S. Sakuragi, M. Kawamura, A. Adachi, Cell-dependent requirement of human immunodeficiency virus type 1 Vif protein for maturation of virus particles, J. Virol. 67 (1993) 1663–1666.

[22] H. Akari, T. Uchiyama, T. Fukumori, S. Iida, A.H. Koyama, A. Adachi, Pseudotyping human immunodeficiency virus type 1 by vesicular stomatitis virus G protein does not reduce the cell-dependent requirement of Vif for optimal infectivity: functional difference between Vif and Nef, J. Gen. Virol. 80 (1999) 2945–2949.

[23] K. Strebel, D. Daugherty, K. Clouse, D. Cohen, T. Folks, M.A. Martin, The HIV 'A' (sor) gene product is essential for virus infectivity, Nature 328 (1987) 728–730.

[24] J.K. Yee, A. Miyanohara, P. LaPorte, K. Bouic, J.C. Burns, T. Friedmann, A general method for the generation of high-titer, pantropic retroviral vectors: highly efficient infection of primary hepatocytes, Proc. Natl. Acad. Sci. USA 91 (1994) 9564–9568.

[25] D.L. Mann, S.J. O'Brien, D.A. Gilbert, Y. Reid, M. Popovic, E. Read-Connole, R.C. Gallo, A.F. Gazdar, Origin of the HIV-susceptible human CD4+ cell line H9, AIDS Res. Hum. Retroviruses 5 (1989) 253–255.

[26] J.S. Lebkowski, S. Clancy, M.P. Calos, Simian virus 40 replication in adenovirus-transformed human cells antagonizes gene expression, Nature 317 (1985) 169–171.

[27] J. Kimpton, M. Emerman, Detection of replication-competent and pseudotyped human immunodeficiency virus with a sensitive cell line on the basis of activation of an integrated β-galactosidase gene, J. Virol. 66 (1992) 2232–2239.

[28] R.L. Willey, D.H. Smith, L.A. Lasky, T.S. Theodore, P.L. Earl, B. Moss, D.J. Capon, M.A. Martin, In vitro mutagenesis identifies a region within the envelope gene of the human immunodeficiency virus that is critical for infectivity, J. Virol. 62 (1988) 139–147.

[29] M. Fujita, A. Sakurai, N. Doi, M. Miyaura, A. Yoshida, K. Sakai, A. Adachi, Analysis of the cell-dependent replication potentials of human immunodefiency virus type 1 *vif* mutants, Microbes Infect. 3 (2001) 1093–1099.

[30] M. Fujita, A. Sakurai, A. Yoshida, M. Miyaura, A.H. Koyama, K. Sakai, A. Adachi, Amino acid residues 88 and 89 in the central hydrophilic region of human immunodeficiency virus type 1 Vif are critical for viral infectivity by enhancing the steady-state expression of Vif, J. Virol. 77 (2003) 1626–1632.

[31] M.K. Karczewski, K. Strebel, Cytoskeleton association and virion incorporation of the human immunodeficiency virus type 1 Vif protein, J. Virol. 70 (1996) 494–507.

[32] K. Nguyen, M. Llano, H. Akari, E. Miyagi, E.M. Poeschla, K. Strebel, S. Bour, Codon optimization of the HIV-1 *vpu* and *vif* genes stabilizes their mRNA and allows for highly efficient Rev-independent expression, Virology 319 (2004) 163–175.

A. 遺伝子診断(genetic diagnosis)

(遺伝学的検査 genetic testing, 遺伝子検査 gene-based testing, 核酸検査 nucleic acid-based testing)

V. 感染症の核酸検査(nucleic acid-based testing)

HIV感染症

HIV infection

足立昭夫

Key words：エイズ，HIV-1，遺伝子診断，遺伝子治療

はじめに

エイズの原因ウイルスであるヒト免疫不全ウイルス1型(human immunodeficiency virus type 1: HIV-1)は1983年に発見された．1986年には第二のヒトエイズウイルス(HIV-2)も同定されたが，世界中に蔓延し人類の脅威となっているのはHIV-1である．アジアやアフリカ地域においては現在もなおHIV-1感染者は非常な勢いで増加し続けている．しかし，この20年間でHIV基礎研究は飛躍的な発展を遂げた．ウイルスゲノムやウイルス蛋白質は詳細に解析され，細胞レベルでのウイルス複製機構は大筋で解明された[1,2]．ウイルスの進化や伝播に関する情報も蓄積され，エイズの予防・治療に密接に関連する分子疫学的研究も進展した[3,4]．現在は，これらを有機的に統合し基礎と臨床をリンクさせた研究が主流となっている．

本稿では，基礎/臨床研究の成果に基づくHIV-1感染の遺伝子診断およびエイズの遺伝子治療について現状を概説する．

1. 概　　念

HIV-1はレトロウイルス科に属するので，基本的にこのウイルス群特有の複製様式に従って増殖する(図1)．ただし，単純なレトロウイルスよりはるかに多い9種の遺伝子をもつため，レンチウイルス属固有の特徴も有している(表1)．個体内でのウイルス増殖は極めて緩やかであるが，次第に体内ウイルス量が上昇し，感染者は徐々にエイズへと進行していく．HIV-1の遺伝子診断や遺伝子治療はこれらの事実に基づいて成立している．

2. 歴史的考察

病原ウイルス感染の有無は，ウイルス分離，ウイルス抗原や核酸の証明および血清学的検査などにより判断される(表2)．ウイルス学あるいは免疫学的手技を用いたウイルス検査・診断は以前から広く行われてきた．検査・診断手法を選択する場合，特異性，迅速性，簡便性，再現性，感度などが重要であり，対象とするウイルスの性質により適切なものが異なることは言うまでもない．HIV-1はその発見直後からゲノム研究が精力的かつ広範囲にわたって行われたので，早い時期から遺伝子診断や遺伝子治療が可能となっていた．

Akio Adachi: Department of Virology, Course of Molecular Medicine, Institute of Health Biosciences, The University of Tokushima Graduate School　徳島大学大学院ヘルスバイオサイエンス研究部 生体制御医学講座 ウイルス病原学分野

0047-1852/05/¥40/頁/JCLS

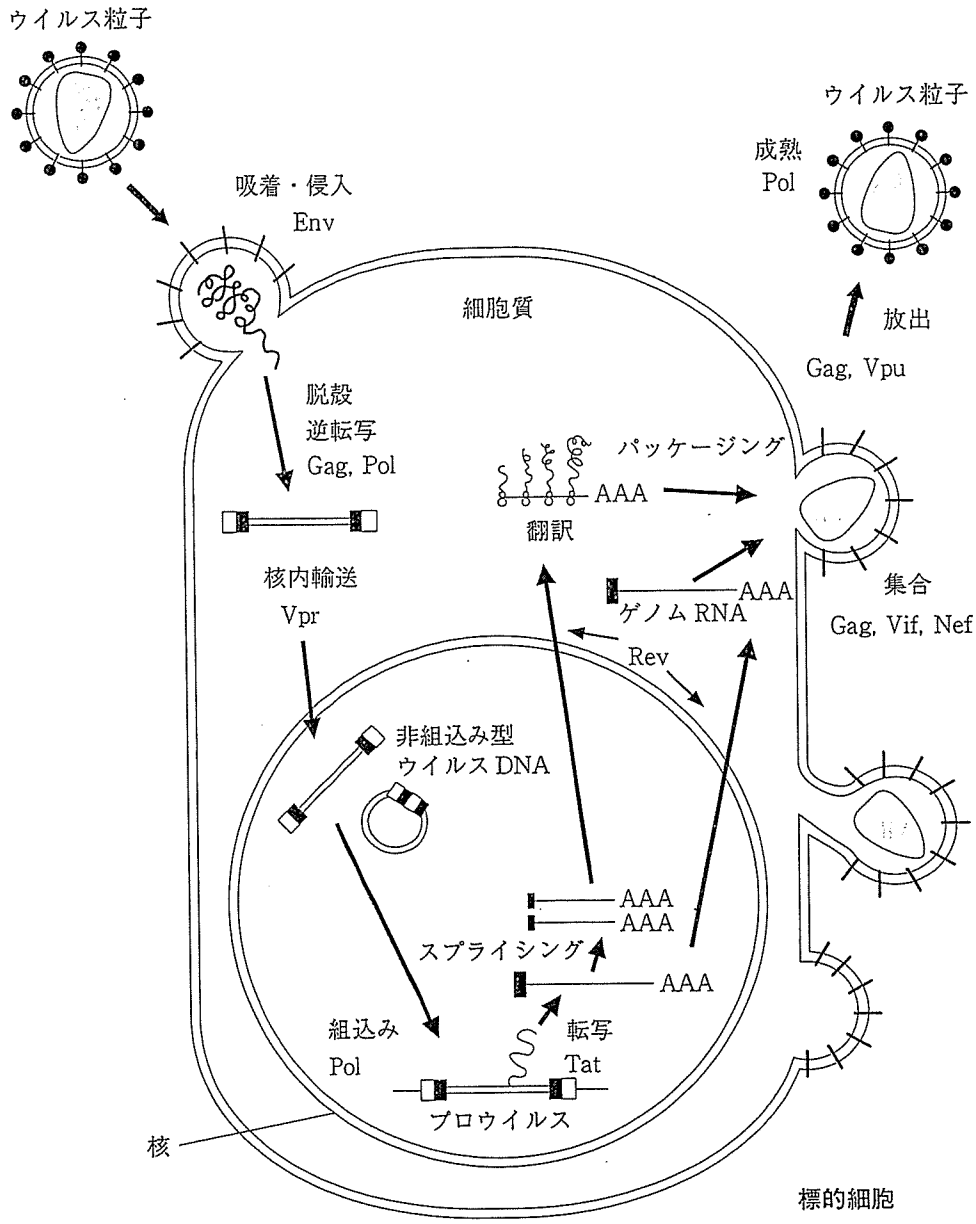

図1 HIV-1の複製サイクル

標的細胞におけるHIV-1複製の各ステップとそれに関与するウイルス蛋白質(表1)を示す．主な標的細胞はCD4陽性Tリンパ球およびマクロファージである．(文献[2]から一部改変して引用)．

3. 遺伝子診断・遺伝子治療

a. 遺伝子診断

HIV-1感染のスクリーニングは，通常抗ウイルス抗体の検出により行われる．迅速検査のための簡便な検査キットも市販されているので，ウェスタンブロット(WB)法による確認検査を含めても短時間でウイルス感染の有無が判定できる[5]．核酸増幅検査(nucleic acid amplification test: NAT)はポリメラーゼ連鎖反応(polymerase chain reaction: PCR)の原理に基づくもので，非常に検出感度が良くかつ定量も容易である[5]．このシステムはHIV-1感染症の検査・診断法として確立している．市販のRT(reverse transcription)-PCRキットにより，血中ウイルス量が測定でき，診断だけでなく個体内のウイルス動態も解析可能となっている．RT-PCR法を用いれば，薬剤抵抗性変異ウイルスの検出も容易

表1 HIV-1蛋白質とその主要な機能

ウイルス蛋白質		機 能
構造蛋白質		
Gag	MA(マトリックス)	ウイルス粒子形成・放出，脱殻・逆転写
	CA(カプシド)	ウイルス粒子形成・放出，脱殻・逆転写
	NC(ヌクレオカプシド)	脱殻・逆転写
	p6	ウイルス粒子放出，Vpr/Vpxのウイルス粒子へのターゲッティング
Pol	PR(プロテアーゼ)	Gag前駆体やGag-Pol前駆体の開裂による成熟ウイルス粒子(感染性ウイルス粒子)の生成
	RT(逆転写酵素)	ウイルスDNA合成(含RNase H活性)
	IN(インテグラーゼ)	ウイルスDNAの細胞染色体DNAへの組込み
Env	gp120	標的細胞受容体への結合
	gp41	標的細胞への侵入
調節蛋白質		
Tat		転写の増強
Rev		構造およびアクセサリー蛋白質(Nefを除く)の発現増強
アクセサリー蛋白質		
Vif		抗ウイルス細胞因子APOBEC3Gの不活化
Vpr		ウイルスDNAの核移行
Vpu		ウイルス粒子の放出促進
Nef		細胞表面におけるMHC-I発現の抑制

表2 病原ウイルスの検査・診断法

検出対象	方 法
感染性ウイルス 感染細胞	培養細胞などへ接種しウイルスを分離 細胞変性効果の観察など
ウイルス粒子	電子顕微鏡による形態の観察，赤血球凝集能測定，特異酵素検出など
ウイルス抗原	蛍光抗体法，ELISA(enzyme-linked immunosorbent assay)，RIA(radioimmunoassay)などによる特異抗原検出
ウイルス核酸	PCR(polymerase chain reaction)あるいはRT-PCR(reverse transcription-PCR)などによる特異核酸の検出
抗ウイルス抗体	ELISA，CF(complement fixation)，HI(hemagglutination inhibition)，WB(Western blot)などによる特異抗体の検出

である．

b. 遺伝子治療

HIV-1感染者の治療法として現在最も有効なものは多剤併用療法(highly active anti-retroviral therapy: HAART)である[6,7]．感染者の体内ウイルスの動態をモニターしつつHAARTを行うことで大きな成果を上げている．しかし，最近の研究から，HAART導入後も潜伏持続感染細胞が減少しないなどウイルス増殖は完全には抑え込めないこと，また，薬剤抵抗性ウイルスの出現も明らかになってきた[6,7]．このため，HIV-1の遺伝子治療は全く新しい治療戦略と

表3 HIV-1感染症の遺伝子治療

抗HIV-1分子	コメント
RNA	
デコイ(decoy)	TatやRevなどの標的配列のデコイを用い，これらによるウイルス複製の増強を阻害する
リボザイム	ウイルス複製に重要なRNA分子を切断して不活化する
アンチセンス	ウイルス複製に重要なmRNAに結合し翻訳を阻害する
siRNA	RNAiによりウイルス複製に重要な細胞(Tsg101，NF-κB，CD4，CCR5など)あるいはウイルス蛋白質(Gag，Pol，Tat，Rev，Vif，Nefなど)の発現を阻害する
蛋白質	
TDN変異蛋白質	結合力はあるが活性がない変異蛋白質(Gag，Tat，Revなど)によって正常ウイルス蛋白質の活性を競合阻害する
細胞内抗体	抗体遺伝子を細胞内で発現させウイルス蛋白質(Env，Tat，Revなど)を不活化する

RNAi: RNA interference(RNA干渉)，siRNA: short interfering RNA，TDN: transdominant negative.

して浮上してきた．ウイルス複製にかかわるウイルスおよび細胞遺伝子(図1)をコントロールすることでHIV-1増殖を抑制しようとする方法である．詳細は他の総説に譲るが[7-10]，表3に主なものをまとめてみた．このうち，RNAi法は現在最も注目されている遺伝子治療である[11]．

4. 将来展望

HIV-1感染症に対する遺伝子診断技術は基本的に確立されているので，今後の課題はその改良である．特に，ウイルスの変異，進化に迅速に対応できるようなシステムの構築が必要とされるであろう．これに対し，HIV-1/エイズに対する遺伝子治療の将来は明るくない．表3に示した抗HIV-1分子はすべて実験室内の細胞レベルでは極めて有効であるが，個体内の標的細胞(HIV-1感染細胞)にいかに効率良く特異的に導入し，発現させるか，この点が大きな未解決の課題となっている．この問題を克服しないかぎり実際の治療には適用困難である．

おわりに

はじめに述べたように，アジア・アフリカ地域でHIV-1感染者は激増している．日本も，先進諸国の中でただ一つ，感染者が増え続けている[12]．HAART法による治療効果は大きいが，根治療法ではなく，抵抗性ウイルスの出現も観察されている．このような状況下では，HIV-1感染を広げないこと，また，個体内や地域に存在するウイルス株を的確に把握することが肝要である．この意味で，HIV-1遺伝子診断は今日ますますその重要性を増しているといえる．

文献

1) 足立昭夫：HIVとその遺伝子機能．ヒトレトロウイルス研究の最前線(山本直樹編)，p13-23，シュプリンガー・フェアラーク東京，2002.
2) 足立昭夫ほか：HIV-1，2．日本臨牀 61(増刊号3)：497-502，2003.
3) 佐藤裕徳，武部 豊：HIVの変異．ヒトレトロウイルス研究の最前線(山本直樹編)，p41-48，シュプリンガー・フェアラーク東京，2002.
4) 照沼 裕：アフリカのAIDS．ヒトレトロウイルス研究の最前線(山本直樹編)，p109-115，シュプリンガー・フェアラーク東京，2002.

5) 今井光信，嶋　貴子：HIV迅速検査．Confronting HIV 2004 no.25，p4-6，ディ・エル・エム・ジャパン，2004.
6) 吉村和久，松下修三：HAARTと潜伏感染．ヒトレトロウイルス研究の最前線(山本直樹編)，p67-74，シュプリンガー・フェアラーク東京，2002.
7) 松下修三：エイズに対する遺伝子治療．感染症の宿主防御機構—理論と実際—(今西二郎編)，p254-263，医薬ジャーナル社，2002.
8) 島田　隆：AIDSの遺伝子治療．AIDS制圧に向けて(高月　清編)，p114-117，医歯薬出版，1996.
9) 明石英雄ほか：RNAiのメカニズム．改訂RNAi実験プロトコール(多比良和誠ほか編)，p16-34，羊土社，2004.
10) 明石英雄ほか：RNAiの応用技術の最新動向—RNAiを用いて何ができるか．改訂RNAi実験プロトコール(多比良和誠ほか編)，p35-44，羊土社，2004.
11) 岡本　尚：RNAi-HIV治療への応用は？ Confronting HIV 2004 no.25，p9-11，ディ・エル・エム・ジャパン，2004.
12) 厚生労働省エイズ動向委員会：国内患者・感染者の届出状況(平成15年エイズ発生動向年報より)．Confronting HIV 2004 no.26，p12-13，ディ・エル・エム・ジャパン，2004.

ELSEVIER

Journal of Neuroimmunology 167 (2005) 108 – 119

Journal of Neuroimmunology

www.elsevier.com/locate/jneuroim

HLA-DRB5*0101 and -DRB1*1501 expression in the multiple sclerosis-associated HLA-DR15 haplotype

Elisabetta Prat [a], Utano Tomaru [a], Lidia Sabater [b], Deric M. Park [a], Rebekah Granger [c], Niels Kruse [d], Joan M. Ohayon [a], Maria P. Bettinotti [e], Roland Martin [a,*]

[a] *Neuroimmunology Branch, National Institute of Neurological Disorders and Stroke, National Institutes of Health, Building 10, Room 5B16, 10 Center DR, Bethesda, MD 20892-1400, USA*

[b] *Laboratory of Immunobiology for Research and Applications to Diagnosis, Centre for Transfusion and Tissue Bank, University Hospital Germans Trias I Pujol, 08916 Badalona, Spain*

[c] *Neuromuscular Diseases Section, National Institute of Neurological Disorders and Stroke, National Institutes of Health, Building 10, 10 Center DR, Bethesda, MD 20892-1400, USA*

[d] *Department of Neurology, University of Würzburg, Josef-Schneider-Str. 11, 97080 Würzburg, Germany*

[e] *Department of Transfusion Medicine/Clinical Center, National Institutes of Health, Building 10, 10 Center DR, Bethesda, MD 20892-1400, USA*

Received 16 November 2004; received in revised form 13 April 2005; accepted 22 April 2005

Abstract

The HLA region, and particularly the DR15 haplotype (containing the two DRB* genes DRB1*1501 and DRB5*0101 and the tightly linked DQ alleles DQA*0102 and DQB1*0602, which together form the DQw6 molecule) in Caucasians, shows the strongest genetic association with multiple sclerosis (MS). In the DR15 haplotype, two β-chains HLA-DRB1*1501 and -DRB5*0101 are co-expressed resulting in two different surface HLA-DR αβ heterodimers, DR2b and DR2a. Most previous studies focused on DRB1*1501, however, both DR2a and DR2b may contribute to MS pathogenesis via antigen presentation to myelin-specific T lymphocytes. We therefore analyzed the expression of the two DR15 genes in various antigen presenting cells (APCs), central nervous system and thymic tissues. Transcript levels were higher for DRB5*0101 in all cell types and tissues. Both HLA-DR heterodimers were expressed at significant levels on the cell surface, where they showed a differential expression pattern in different APCs. They were similarly regulated after stimulation with interferon-γ and interleukin-4. Finally, immunohistochemistry experiments indicated that both molecules were expressed in thymic tissue. Our results encourage future research to investigate the potential functional relevance of both genes for the pathogenesis of MS.

Keywords: MHC; Multiple sclerosis; Antigen presenting molecules; Antigen presenting cells

1. Introduction

Multiple sclerosis (MS) is considered a T cell-mediated autoimmune disease that is triggered by an as yet unknown foreign agent in genetically susceptible individuals (Martin et al., 1992). Epidemiological and genetic studies, including several whole genome searches (Dyment et al., 2004), provide evidence that MS is genetically complex, i.e. a number of different genes contribute to disease susceptibility (Wandstrat and Wakeland, 2001), and among these, genes of the major histocompatibility complex (MHC; HLA in humans) region show the strongest association. In Caucasian MS patients, the genes of the HLA-DR15 haplotype are the closest associated with disease (Vartdal et al., 1989), and studies of cellular immune responses against myelin antigens (Martin et al., 1992) favor DR alleles as the most relevant.

HLA-DR molecules are heterodimers composed of a highly polymorphic β-chain encoded by DRB1* or DRB3-5* genes associated with a nonpolymorphic α-chain encoded by the DRA1*0101 gene. In most haplotypes, two HLA-DRB genes are expressed, one of the DRB1*

* Corresponding author. Tel.: +1 301 594 9084; fax: +1 301 402 0373.
E-mail address: martinr@ninds.nih.gov (R. Martin).

0165-5728/$ - see front matter © 2005 Elsevier B.V. All rights reserved.
doi:10.1016/j.jneuroim.2005.04.027

locus and one of the loci encoding DRB3*, -4*, or -5*. Consequently, two non-allelic HLA-DR molecules are expressed on the cell surface. In the MS-associated HLA-DR15 haplotype, the two β-chains, HLA-DRB1*1501 and DRB5*0101, together with DR-α result in the two functional surface heterodimers, DR2b (DRA*0101, DRB1*1501) and DR2a (DRA*0101, DRB5*0101) (Vergelli et al., 1997b). In this report, we will use the terms DR2b and DR2a and HLA-DRB1*1501 and -DRB5*0101 interchangeably, even though the latter only refer to the polymorphic DR-β chain genes.

Most studies on the role of HLA-class II molecules in MS examined DRB1*1501, however, some paid attention to the above mentioned co-expression of DR2a and DR2b, and showed that both molecules can serve as restriction elements for myelin basic protein (MBP)-specific T cells (Jaraquemada et al., 1990; Martin et al., 1991; Ota et al., 1990; Pette et al., 1990; Vergelli et al., 1997b) or autoreactive T cells in general. Due to differences in their peptide binding properties, a different spectrum of MBP peptides is presented by DR2a versus DR2b (Vergelli et al., 1997b). Furthermore, in addition to serving as antigen presenting molecules for MBP-specific T cells (Jaraquemada et al., 1990; Vergelli et al., 1997b), the restriction element, i.e. DR2a versus DR2b, may also influence T cell effector functions: DR2a-restricted MBP-specific T cell clones are highly cytotoxic, mediating high-efficiency lysis by perforin, while DR2b-restricted clones mediate low-efficiency lysis via Fas–Fas–ligand interaction (Vergelli et al., 1997a).

It has been described for several HLA DR haplotypes, that the DRB1* gene is differentially expressed from the DRB3*-4*, -5*-encoded beta chain (Berdoz et al., 1987; Cotner et al., 1996; Emery et al., 1993). Furthermore, the level of DR molecule expression is important for the activation of T lymphocytes (Matis et al., 1983), e.g.: increased HLA class II expression could lead to enhanced antigen presentation via increased ligand density (Bontrop et al., 1986), and stronger T cell activation.

In light of the above, we investigated the expression of both DR2a and DR2b. We believe that this data on HLA-DR15 haplotype will encourage future research to investigate the influence of both DR2a and DR2b in MS pathogenesis. We analyzed the mRNA and surface expression of the two genes in peripheral blood mononuclear cells (PBMCs), B cells, monocytes, dendritic cells, activated T cells, cerebrospinal fluid (CSF) cells, and central nervous system (CNS) and thymic tissues obtained from healthy donors (HDs) and MS patients.

2. Materials and methods

2.1. Subjects

The study population consisted of 22 HLA-DR15 positive subjects: 8 HDs and 14 patients with clinically definite MS (7 females and 7 males), of whom 9 were affected by relapsing–remitting MS and 5 by secondary-progressive MS. Seven MS patients were not on therapy, while seven received Interferon β-1a or -1b. MS patients did not receive any immunosuppressive therapy for a period of 3 months prior to the study. Thirteen HLA-DR15 negative subjects, three MS patients and ten HDs, were studied as negative controls. Blood and CSF were obtained under a National Institute of Neurological Disorders and Stroke Institutional Review Board (IRB)-approved protocol. HLA-typing for HLA-A, -B, -C and -DR, -DQ was performed at the Department of Transfusion Medicine, NIH, by molecular HLA typing techniques. The method used was sequence specific primer-PCR amplification of genomic DNA (Player et al., 1996).

2.2. Cell cultures and cell isolation techniques

PBMCs were separated from leukaphereses by density gradient centrifugation (Lymphocyte Separation Medium, Bio Whittaker, Walkersville, MD). Monocytes and B cells were purified from PBMCs, respectively, by adherence to plastic and negative selection using the MACS B cell Isolation Kit (Miltenyi, Auburn, CA). Dendritic cells (DCs) were generated from monocytes using a well-established sequential cytokine treatment as previously described (Thurner et al., 1999). CSF cells were obtained by lumbar puncture from 2 MS patients. Bare lymphocyte syndrome (BLS) cells transfected with HLA-DRB5*0101 (BLS-DR2a), -DRB1*1501 (BLS-DR2b), -DRB1*0401 (BLS-DR4) and -DQB1*0602 (BLS-DQw6) were kindly provided by Dr. W.W. Kwok and Dr. G. Nepom (Benaroya Research Institute, University of Washington, Seattle, WA).

2.3. CNS tissues

Blocks of frozen CNS tissues containing MS lesions were obtained from 7 HLA-DRB1*1501 and -DRB5*0101-positive patients (6 females and 1 male; average duration of disease: 13 years) during autopsy and were kindly provided by Dr. C. Raine (Albert Einstein College of Medicine, New York, USA).

2.4. Thymic tissue samples

Thymic tissue samples were obtained under an IRB-approved protocol (University Hospital "Germans Trias i Pujol", Badalona, Spain) by thoracic surgery at University Hospital Valle de Hebron (Barcelona). Molecular typing was performed on tissue samples to identify HLA-DR15 positive subjects. Thymus 1 was obtained from a 6-year-old subject affected by Down syndrome, thymus 2 from a 69-year-old subject affected by Graves disease, thymus 3 from a 69-year-old subject affected by myasthenia gravis.

2.5. Cytokines and antibodies

Interleukin (IL)-4 and interferon (IFN)-γ were obtained from PeproTech (Rocky Hill, NJ), phytohemagglutinin (PHA) from Sigma (St. Louis, MO) and IFN-β1b from Berlex Laboratories (Richmond, CA). Purified mouse anti-DRB1*1501 (PUH0596) and anti-DRB5*0101 (PUH0427A) IgM monoclonal antibodies (Abs) were purchased from One Lambda Inc. (Canoga Park, CA) under an agreement between One Lambda Inc. and the National Institutes of Health. The same Abs were custom conjugated, respectively, with Alexa Fluor 594 and 488 by Molecular Probes (Eugene, OR) and used for immunofluorescence studies on thymic tissue frozen sections. Anti-DRα Ab (L243) was purchased from ATCC (Rockville, MD) and purified ascites generated by Biocon (Rockville, MD). Additional Abs used during the course of FACS analysis experiments were: goat–anti-mouse IgM and anti-mouse IgG R-Phycoerythrin (PE)-labeled Abs (Jackson ImmunoResearch Laboratories, West Grove, PA), CD11c, CD14, CD86, CD80, CD54, CD1a, CD40, CD19, CD45, CD3 (BD PharMingen, San Diego, CA), CD83 (Immunotech, Marseille, France); isotype controls: mouse IgM, IgG2a, IgG2b, IgG1k, were purchased from Caltag (Burlingame, CA) or from BD PharMingen.

2.6. Reverse transcription and real-time polymerase chain reaction (RT-PCR)

RNA was extracted using RNeasy Mini Kit (Qiagen, Valencia, CA). For each sample, 500 ng of total RNA was reverse-transcribed in 50 μl reaction volume using TaqMan Gold RT-PCR Kit (Applied Biosystems, Foster City, CA) with random hexamers.

The TaqMan 5′ nuclease fluorogenic quantitative PCR assay was performed using the ABI 7700 System (PE Applied Biosystems). Primers and probes for DR2a and DR2b genes were in part modified from Albis-Camps and Blasczyk (1999) or newly designed using Primer Express 1.0 (ABI, Applied Biosystems). Oligonucleotides were placed in polymorphic regions of the genes for maximal specificity. Forward and reverse primers for each set were positioned in exons 1 and 2, respectively, to prevent amplification of contaminating genomic DNA. Primers/probes sequences were the following: DR2a forward primer: 5′ TGGAGGTTCCTACATGGCAAA 3′; DR2a reverse primer: 5′ GCTGTCGAAGCGCAAGTC 3′; DR2a probe: 5′ FAM-TGCGGTTCCTGCACAGAGACATCTATAACC-TAMRA 3′; DR2b forward primer: 5′ AGCTCCCCACT-GGCTTTGT 3′; DR2b reverse primer: 5′ TCCACCGCG-GCCCGCGC 3′; DR2b probe: 5′ FAM-TGCTCCAGGA-TGTCCTTCTGGCTGTT-TAMRA 3′. Primer and probe sequences for the housekeeping gene, human β-actin, were chosen to span exon junctions (Kruse et al., 1997). Since the main goal of this study was to compare the expression levels of DR2a and DR2b, which are co-expressed in the same cell, internal calibration was not essential and human β-actin was considered a suitable calibrator. Real-time PCR assays were conducted using Platinum Quantitative PCR SuperMix-UDG (Gibco BRL, Life Technologies, Carlsbad, CA). $MgCl_2$ and primer and probe concentrations were optimized as described (AppliedBiosystem, 1998).

2.7. DNA plasmid and standard curve preparation

To quantify the mRNA expression of DR2a and DR2b genes, standard curves were prepared using linearized plasmid DNA for HLA-DRB5*0101, HLA-DRB1*1501 and human β-actin (Kruse et al., 1997). Plasmid standard curves were generated performing 10 serial, three-fold dilutions. Each dilution was measured in triplicate in each PCR experiment. The logarithmic value of the initial plasmid target copy number was plotted versus threshold cycle value for each dilution and a linear relationship was detected: in all experiments $R^2 > 0.993$. DR2a, DR2b primer/probe combinations could reliably detect as few as 80 and 40 input copies/reaction, respectively. The efficiencies of the reaction on plasmid DNA and on sample cDNA were comparable, so plasmid materials proved to be a suitable standard for quantitation. The copy number of DR2a, DR2b and β-actin in each sample was calculated based on the respective plasmid standard curves. DR2a and DR2b were then normalized to β-actin.

2.8. Specificity of RT-PCR assay

Based on sequence similarities, we considered that DR2b and DR2a primers/probes were potentially cross-reactive, respectively, with DRB1*1502, *1503, *1506, *1507, *1509 and with DRB5*0104, *0106, *0107 and *0109. Knowing the HLA-typing of donors, we were able to exclude from the study those carrying these alleles. Furthermore, real-time PCR experiments were performed on BLS-DR4, -DQw6 and on 13 cDNA samples obtained from PBMCs of HLA-DR15 negative donors: they were all negative. Additionally, DR2a and DR2b oligonucleotides did not recognize, respectively, DR2b and DR2a transcripts when tested on BLS-DR2b and -DR2a cells and on plasmid material. Control PCR reactions were performed on non-reverse-transcribed RNA to exclude any contamination by genomic DNA. Primers did not share sequence identity with DRB pseudogenes.

2.9. Accuracy of real-time RT-PCR

The intra-assay coefficient of variance (CV)% (i.e.: SD/Average × 100) of threshold cycle values of the DR2a and DR2b real-time PCR assay was between 0.1% and 0.9%. The DR2a/DR2b ratio intra-assay CV% reflecting the variability introduced by the RNA extraction procedure, the RT reaction, and the real-time PCR assay was on average 8.5%. The inter-assay CV% of threshold cycle

values of the PCR reaction performed on cDNA material was 1.3% and 2.4% for DR2a and DR2b, respectively. Similar values were obtained when the reaction was performed on plasmid DNA standards.

2.10. Flow cytometry staining for DR2a and DR2b

Cells were incubated on ice for 30 min with Ab diluted in cold staining buffer (phosphate-buffered saline, 5% fetal bovine serum, 0.1% sodium azide). Before and after incubation, cells were washed twice in staining buffer and immediately analyzed by flow cytometry. Two-color analysis was performed on a FACScan™ using CellQuest software (Becton-Dickinson, San Jose, CA), acquiring 5000 events for each condition based on forward/side scatter parameters.

2.11. Immunofluorescence staining for DR2a and DR2b in tissue sections

Cryostat sections (10 μm) were air dried for 2 h, fixed in ice-cold acetone for 20 min and washed 3 times in PBS. Sections were then incubated for 2 h with Ab in a humidified container. After washings with PBS, sections were mounted in SlowFade Light Antifade Kit with DAPI reagents (Molecular Probes) and viewed with Zeiss Axiovert 200M microscope (Carl Zeiss, NY) using appropriate filters. Single-, double- and triple-color images were digitally captured by a high-resolution CCD camera using AxioVision 3.1 software (Carl Zeiss).

2.12. Specificity and affinity of anti-DR2a and -DR2b antibodies for flow cytometry and immunofluorescence staining

The specificity of anti-DR2a and -DR2b Ab was tested using isotype control Abs and BLS-DR2a, -DR2b, -DR4 and -DQw6 cells, as well as PBMCs obtained from HLA-DR15 negative donors. In particular, for immunofluorescence staining, the Ab specificity was tested using purified isotype control and specific Ab in indirect staining because a directly labeled isotype control Ab was not commercially available. Furthermore, a mixture of BLS-DR2a and -DR2b cells was incubated with the two directly labeled anti-DR2a and -DR2b Abs. The two cell populations were easily distinguishable by the different fluorochromes (Fig. 5b). Ab titrations were conducted to establish saturating concentrations in flow cytometry. As a difference in the affinity between the two Abs may bias the estimation of fluorescence intensity (FI) levels in flow cytometry, L243 (anti-DRα) Ab, a monomorphic anti-DR Ab reacting with DR-alpha and recognizing both DR2a and DR2b, was used to normalize the signals obtained with the two specific Abs. The ratios: specific Ab-mean FI (-MFI) or -geometric MFI

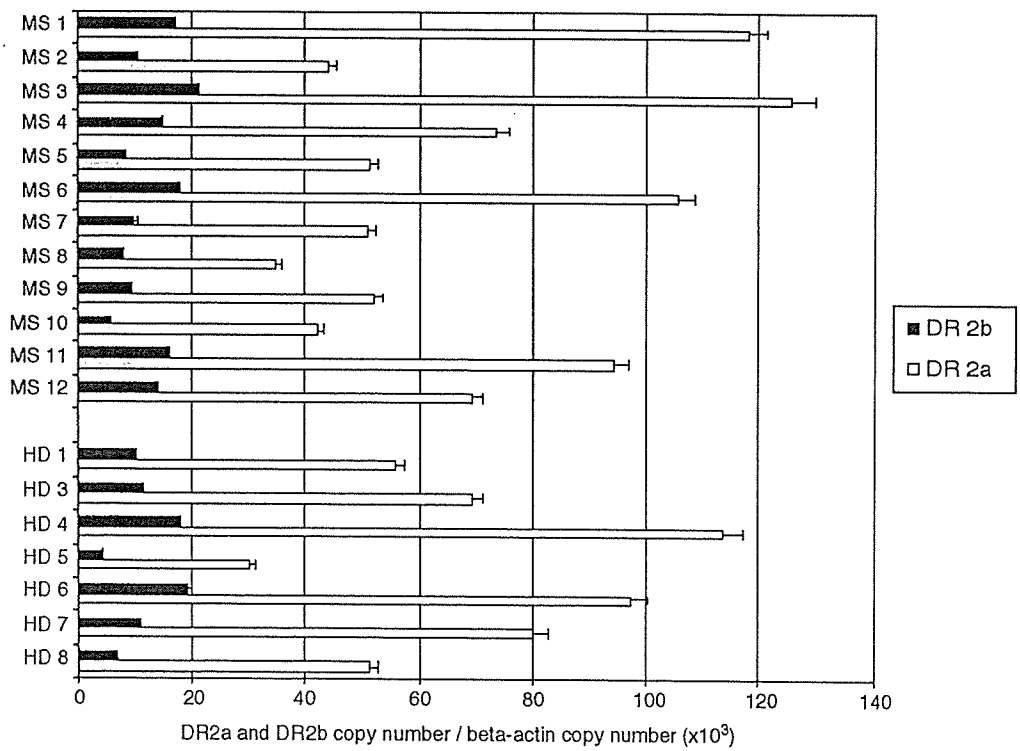

Fig. 1. Relative expression of DR2a and DR2b mRNA in PBMCs obtained from 12 MS patients and 7 HDs. RNA was reverse transcribed and amplified for DR2a and DR2b by real-time PCR. Levels of RNA were normalized to human β-actin. Data are presented as mean of triplicate values±SD. MS: multiple sclerosis patient, HD: healthy donor.

(-geo.MFI)/L243-MFI or -geo.MFI were calculated for anti-DR2a and -DR2b Ab during the course of repeated experiments on BLS-DR2a or -DR2b cells, respectively. The relative affinity of the anti-DR2a Ab was higher than that of anti-DR2b Ab, and therefore we applied correction factors to all flow cytometry data.

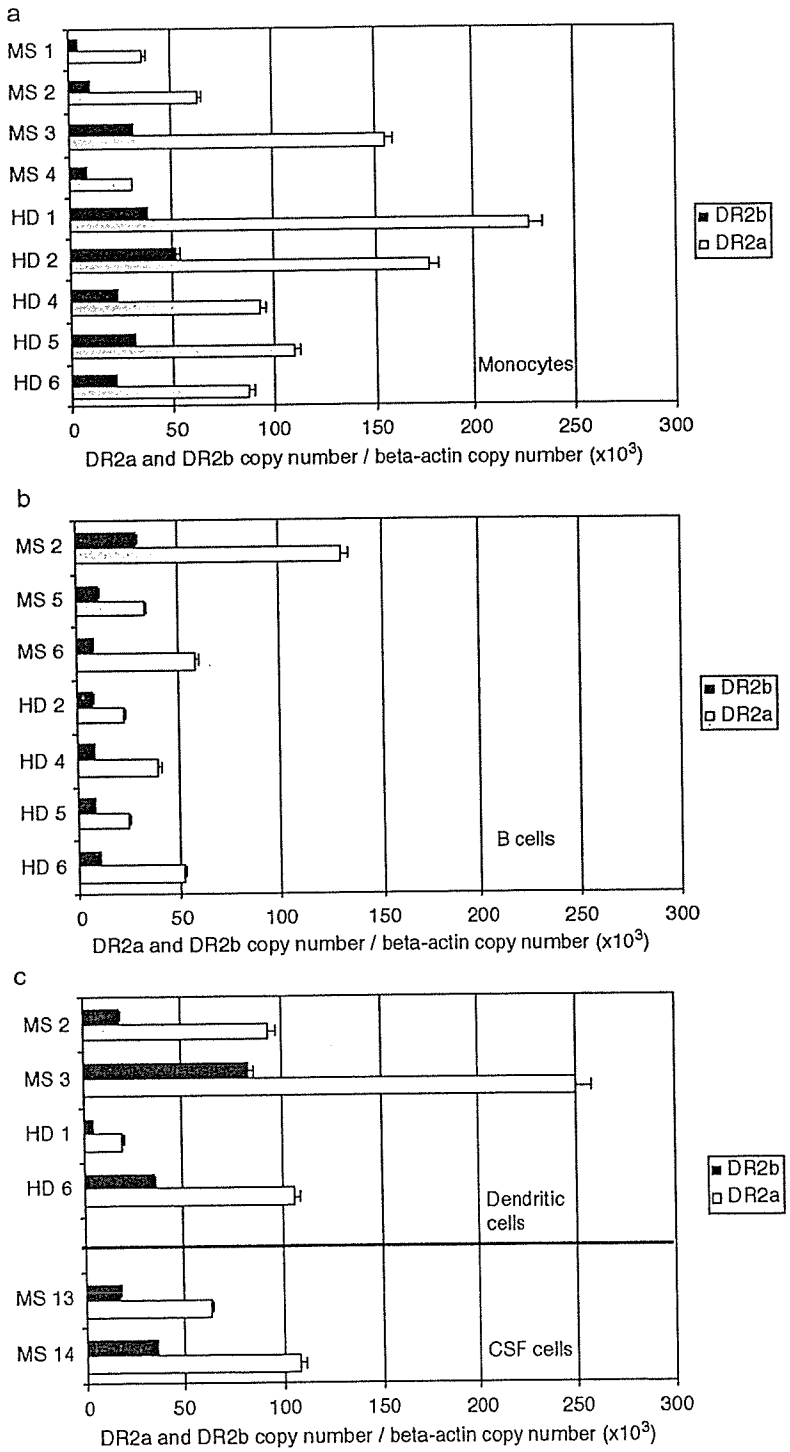

Fig. 2. Relative expression of DR2a and DR2b mRNA in monocytes (a), B cells (b), dendritic cells and CSF cells (c).

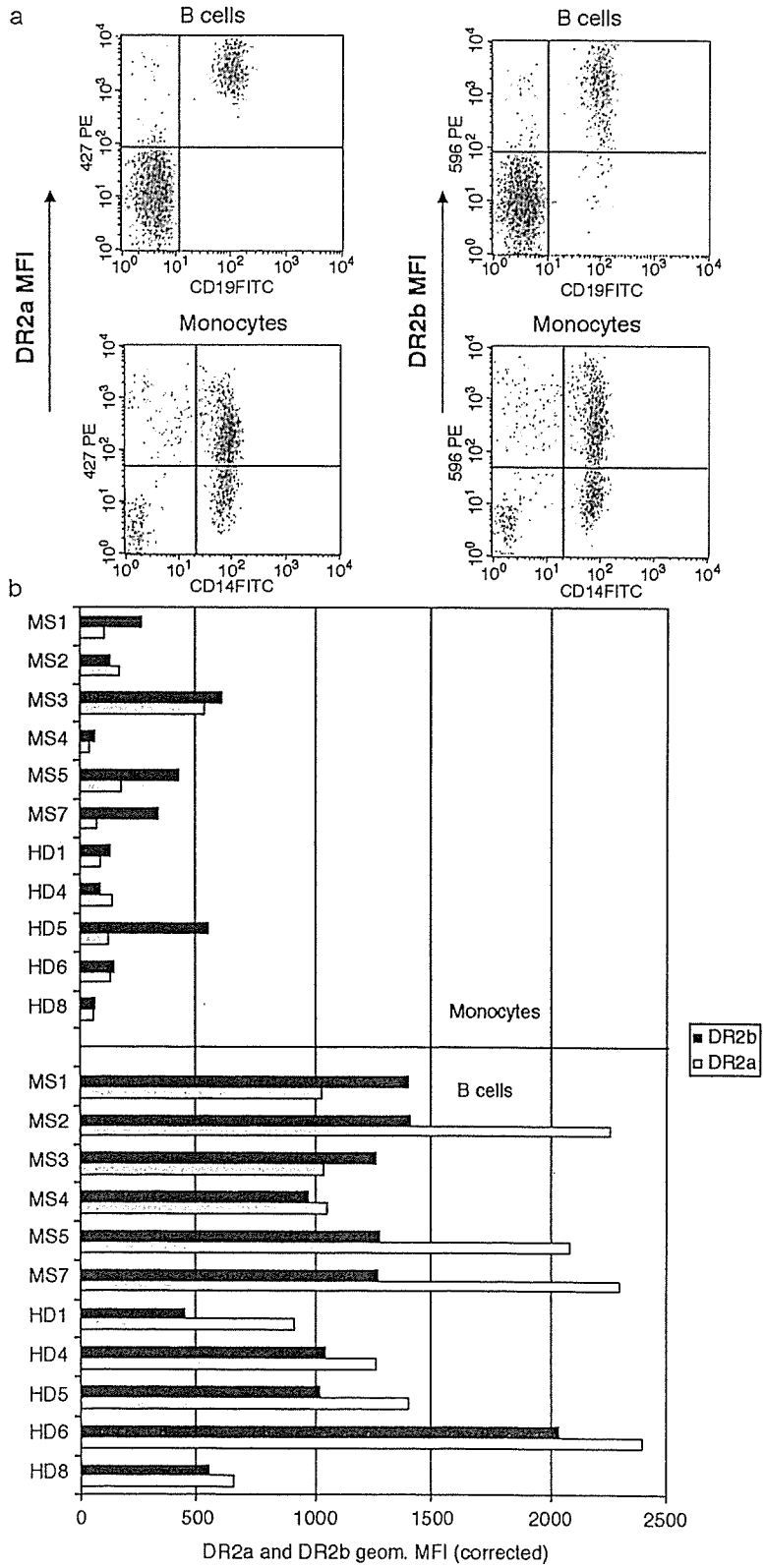

Fig. 3. DR2a and DR2b surface staining on B cells, monocytes and dendritic cells. (a) Representative staining profiles of DR2a and DR2b on B cells (CD19 positive cells) and monocytes (CD14 positive cells). (b) DR2a and DR2b geometric MFI (geom.MFI) values of monocytes and B cells obtained from 6 MS patients and 5 HDs. Geom.MFI values were corrected for the different affinity of the two Abs. (c) DR2a and DR2b MFI values of the same dendritic cells in Fig 2c.

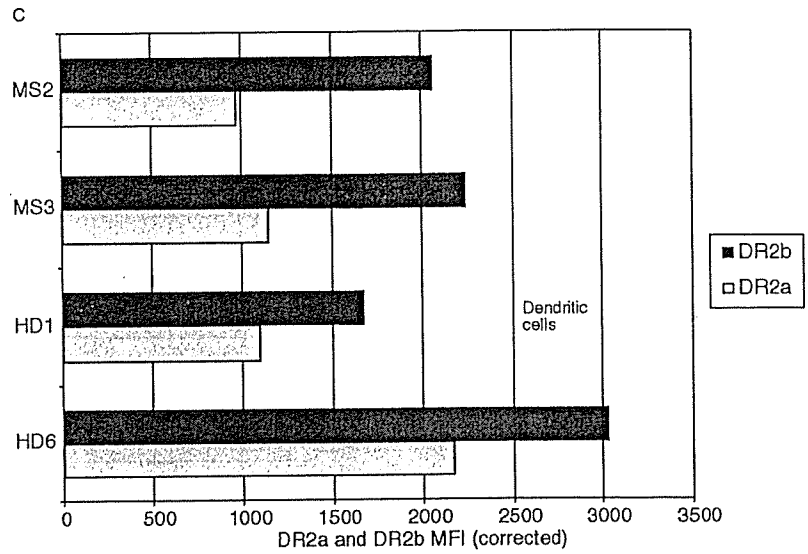

Fig. 3 (*continued*).

2.13. Statistical analyses

Statistical analyses were performed using SigmaStat 2.03 statistical analysis software. Wilcoxon signed-rank test or Wilcoxon rank-sum test was used where appropriate.

Values are expressed as average of DR2a/DR2b transcript or protein levels ratios ± SD.

3. Results

To quantitate the mRNA expression of DR2a and DR2b, we developed a real-time RT-PCR assay and tested its specificity, sensitivity and accuracy as outlined in Materials and methods. Furthermore, we described the methods to assess the specificity and affinity of the two monoclonal Ab that were used to evaluate the surface expression of the two DR molecules by flow cytometry and immunohistochemistry. We subsequently analyzed DR2a and DR2b expression in different APCs and tissues obtained from HDs and MS patients.

3.1. PBMCs

DR2a and DR2b mRNA expression was studied on PBMCs obtained from 12 MS patients and 7 HDs (Fig. 1). DR2a expression was 5 ± 0.8 ($p = 0.001$) times higher than DR2b expression.

3.2. Monocytes, B cells and dendritic cells

Monocytes and B cells were subsequently purified from the PBMCs of a total of 11 donors, 6 MS patients and 5 HDs. On average, transcripts were 4.9 ± 1.6 ($p = 0.004$) (monocytes, Fig. 2a) and 4.3 ± 0.5 ($p = 0.016$) (B cells, Fig. 2b) times higher for DR2a than for DR2b.

Dendritic cells were generated from 2 MS patients' and 2 HDs' monocytes. DR2a mRNA expression was on average 3.7 ± 0.9 times higher than DR2b expression (Fig. 2c).

To study the surface expression of the two molecules, 6 MS patients' and 5 HDs' PBMCs were stained with anti-DR2a and -DR2b Ab. B cell and monocyte populations were identified by gating on CD19+ and CD14+ cells, respectively. As shown in a representative experiment in Fig. 3a, all B cells expressed DR2a at high levels, while DR2b expression varied in intensity across the cell population. In monocytes, the expression varied widely for both alleles, in particular for DR2b. In light of this distribution pattern, we considered that the geometric MFI (geo.MFI) was the best parameter to compare DR2a and DR2b expression in B cells and monocytes. Both DR2a and DR2b were expressed at significant levels on the surface of B cells and monocytes. However, the DR2a geo.MFI value was higher than that of DR2b in 9/11 donors' B cells, and it was on average 1.3 ± 0.4 ($p = 0.042$) times that of DR2b (Fig. 3b). In monocytes, the geo.MFI value of DR2b was higher than that of DR2a in 9/11 donors, and it was on average 2 ± 0.4 ($p = 0.032$) times the expression of DR2a (Fig. 3b).

Similarly to monocytes, dendritic cells surface expression was 1.8 ± 0.3 times higher for DR2b than for DR2a (Fig. 3c).

When comparing the ratio of DR2b/DR2a expression levels between MS patients and HDs, no differences were observed.

To investigate whether DR2a and DR2b expression was differentially modulated by known MHC inducers, we studied their temporal expression in monocytes and B cells

from both HDs and MS patients upon stimulation with 500 U/ml IFN-γ and 20 ng/ml IL-4, respectively. Titrations were performed and the above IFN-γ and IL-4 doses proved to be the most effective for in vitro experiments. A total of 10 time course (24, 48 and 72 h) experiments were performed. The expression of the two alleles was similarly modulated both at the mRNA and surface level (not shown).

3.3. T cells

As activated T cells are able to express MHC class II molecules and may play a role in antigen presentation in addition to professional APCs, we studied DR2a and DR2b surface expression on activated T cells. PBMCs were incubated with 2.5 μg/ml PHA. After 48 h of incubation, DR2a and DR2b surface expression was evaluated on CD3+ T cells: both molecules were up-regulated in about 65% of T cells and their surface expression was 1.6 times higher for DR2b compared to DR2a (not shown).

3.4. Response to IFN-β

We also wanted to study whether DR2a and DR2b expression can be differentially down-modulated. As previously reported, IFN-β, one approved therapy of MS, down-regulates the MHC class II expression induced by IFN-γ in macrophages, B cells and human glial cells (Fertsch et al., 1987; Inaba et al., 1986; Jiang et al., 1995). Therefore, PBMCs were incubated with IFN-β (1000 U/ml) or IFN-γ (100 U/ml), respectively, or a combination of the two, or medium only. DR2a and DR2b surface expression was studied by flow cytometry in B cells. The treatment with IFN-β resulted in an approximately 40% reduction in both HLA-DR2a and DR2b expression induced by IFN-γ (not shown). We did not observe lower levels of DR2a and DR2b surface expression in MS patients that were treated with IFN-β. This is not surprising since in our in vitro experiment IFN-β was used at concentrations higher than those achievable in vivo.

3.5. Cerebrospinal fluid cells

We analyzed DR2a and DR2b mRNA expression in 2 CSF mononuclear cell samples from MS patients. DR2a was on average 3.2 times higher expressed than DR2b (Fig. 2c).

3.6. CNS tissues

In CNS tissues DR2a mRNA expression was on average 5±1.8 ($p=0.001$) times higher than that of DR2b (Fig. 4).

3.7. Thymic tissue

The thymus is the central immune organ for cellular immune responses and the site of negative and positive selection. As thymic expression of DR2a and DR2b may be important for the development of central tolerance, we analyzed the expression of the two molecules in 3 thymic tissue samples. DR2a mRNA expression was on average 3.5±0.5 times higher than that of DR2b (Fig. 5a). Immunofluorescence staining on frozen sections obtained from the same 3 thymic tissue samples showed that both alleles were clearly expressed (Fig. 5c, d, e). Further studies are necessary to follow up on the preliminary observation of a differential distribution of DR2a and DR2b surface expression in thymic tissue that could not be

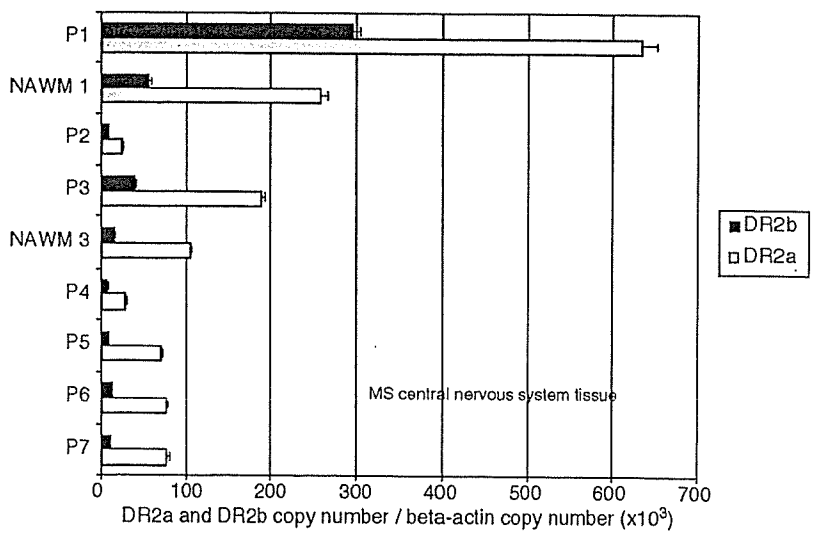

Fig. 4. Relative expression of DR2a and DR2b mRNA in MS lesion containing material obtained from 7 patients. NAWM: normal appearing white matter; P: MS lesion containing material.